JOURNAL OF MATERIALS SCIENCE 32 (1997) 4613–4617

The falling weight impact properties of maleic anhydride compatibilized polypropylene–polyamide blends

S. C. TJONG
Department of Physics and Materials Science, City University of Hong Kong, Tat Chee Avenue, Kowloon, Hong Kong

A series of polypropylene–polyamide 6 (PP–PA) blends of composition 80:20, 50:50 and 20:80 have been prepared in a twin screw extruder followed by injection moulding. Maleic anhydride grafted polypropylene was used as a compatibilizer for these blends. Static mechanical and falling weight impact tests were performed on these blends. The fracture surfaces of impact specimens were subsequently examined by scanning electron microscopy (SEM). The mechanical properties of the blends were found to be strongly dependent on the PP–PA blend ratios. The Young's modulus, tensile strength and impact energy were observed to increase with increasing PA content. The impact strength was better in blends when the PA content approached 80 wt %. SEM observations revealed that the addition of compatibilizer resulted in good adhesion between the PP dispersed domains and PA matrix in the PP–PA 20:80 blend. Furthermore, the SEM fractographs also indicated that the cold drawn of PA matrix and debonding of PP domains were responsible for the high impact strength of this blend.

1. Introduction

Research into polymer blends generally involves matrix polymers that are easily attainable from commercial sources. Polypropylene (PP) and polyamide (PA) are two major commodity thermoplastics that are readily available and produced in large quantities. PP is characterized by its high melting temperature, high elongation-to-break, good moisture resistance and low cost, but it suffers from relatively low strength and poor chemical and heat resistance. On the other hand, PA exhibits high tensile strength and it is strongly resistant to most solvents. PA normally has a high affinity for water, and its mechanical properties are often significantly affected by the absorption of water. Thus PA is frequently blended with lower modulus polymers such as polyolefins to improve materials properties [1–7]. The addition of PP lowers water absorption and reduces materials cost.

PP–PA polymer blends have previously been reported to be immiscible [3, 6]. The size and the shape of the dispersed phase are important factors that determine the mechanical properties of the blends. Blend morphology is dependent on a number of factors, e.g. composition, viscosity ratio, interfacial tension and the processing conditions [3, 8]. These factors may determine which of the components is the dispersed phase and where phase inversion would occur. The inherent incompatibility between PP and PA has been a limiting factor in achieving good impact performance and high tensile strength of the blends. Significant improvement in blend properties can usually be achieved by the addition of the compatibilizing agents that are mostly polyolefins functionalized with maleic anhydride or acrylic acid [5, 9, 10]. These functional groups react with the amine groups of the polyamide, giving rise to strong links between the two phases. The morphology, static tensile properties and fabrication of PP–PA compatibilized blends have been investigated by several workers [5, 6, 11, 12]. They reported that the compatibilizing tends to promote interfacial adhesion and to produce much finer dispersed phase domains in PP–PA blends. Thus, the addition of compatibilizing agents results in improvements of the tensile and Izod impact properties of PP–PA blends. This paper investigates the morphology and falling weight Charpy impact properties of the maleic anhydride compatibilized PP–PA blends.

2. Experimental procedure

The polypropylene used was Profax 633/Melt Flow Index (MFI = 29/10 min) supplied by Himont. The maleic anhydride grafted polypropylene copolymer (PP-g-MA) used was Hercoprime (5% function group) supplied by Himont. Polyamide-6 (PA6) was G1018 obtained from WBE Industries (Japan). The raw materials were in the form of pellets. The compositions of PP–PA6 blends (by weight) examined were 100:0, 80:20, 50:50, 20:80 and 0:100. These blends were prepared by mixing the well dried pellets thoroughly,

0022–2461

followed by melt mixing in a corotating twin screw extruder (Brabender Plasticoder) operating at 220–270 °C. The PP–PA6 blends were compatibilized by adding 6 wt % PP-g-MA. The strands of the extrudates were chopped in a granulator to obtain pellets with an average size of ~4 mm. These pellets were dried in the oven for 2 h prior to injection moulding. Using these pellets, dog-bone shaped tensile bars (ASTM D638) were injection moulded.

Static mechanical properties of the injection moulded bars were determined using an Instron tensile tester (model 4206) at a cross-head speed of $2\,mm\,min^{-1}$. In the falling weight Charpy impact tests, rectangular specimens with dimension of $75 \times 13 \times 3\,mm^3$ were prepared from the gauges section of the injection moulded tensile bars. The notch length was 2.5 mm. A Ceast Fractovise instrumental falling weight system was used to perform the impact tests. The impactor was equipped with an instrument tup and the signal was fed to a data acquisition board in a spectrum system computer; thus the computer can record a load–displacement curve of the impact fracture. The mass of the striker was 3.164 kg and the free clearance was 52 mm. The fracture surfaces of the specimens after impact tests were examined in a scanning electron microscope (SEM). These surfaces were coated with a thin layer of gold prior to SEM observations.

3. Results and discussion

Figs 1 and 2 show the variation of tensile modulus and tensile strength of the PP–PA6 blends versus PA6 content, respectively. These figures indicate that both the tensile modulus and strength of the blends are increased as the PA6 content increases. Thus improvement in the tensile properties appears to take place when the continuous PP phase is replaced by continuous PA phase.

Fig. 3 shows a typical falling weight impact load–time curve of the pure PP specimen. The PP specimen fractures in a brittle mode as seen from the impact energy and a nearly triangular shape load–unloading form with no propagation energy. Fig. 4 shows the falling weight impact strength of the PA6 and PP specimens as a function of velocity. It can be seen that the impact strength of PA6 tested at various impact speeds is generally much higher than that of PP. Furthermore, the impact strength of the PA6 specimen tends to drop dramatically when the impact velocity is increased from 1 to $4.4\,m\,s^{-1}$. In this case, the impact strength is decreased from 9.142 to $6.0\,kJ\,m^{-2}$. Polyamides are known to be notch-sensitive thermoplastics arising from a significantly lower resistance to crack propagation than crack initiation. In this case the polyamides are brittle at high strain rates. On the other hand, the impact strength of PP also appears to decrease with increasing velocity [12] but the reduction in impact strength of PP with velocity is considerably smaller when one compares it to PA6.

Fig. 5 shows the falling weight impact strength of various PP–PA6 blends as a function of impact velocity. This figure indicates that the polymer blends containing up to 50% PA6 have a relatively low impact strength. However, the impact strength is better in blends where the PA weight fraction is 0.8. The effect of PA concentration on the impact strength of PP–PA blends tested at velocities of 1 and $4.05\,m\,s^{-1}$ is summarized in Fig. 6a and b.

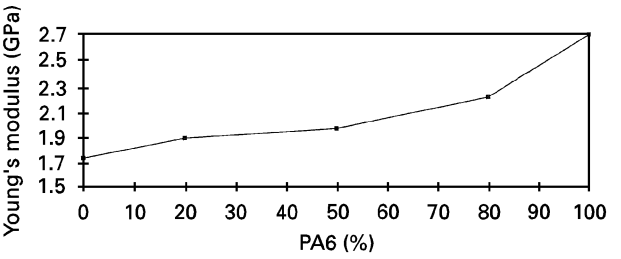

Figure 1 Variation of tensile modulus of PP-PA6 blends versus PA content.

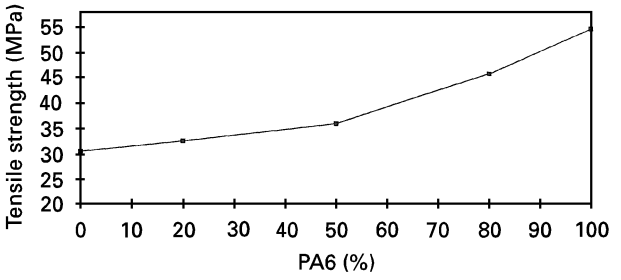

Figure 2 Variation of tensile strength of PP-PA6 blends versus PA content.

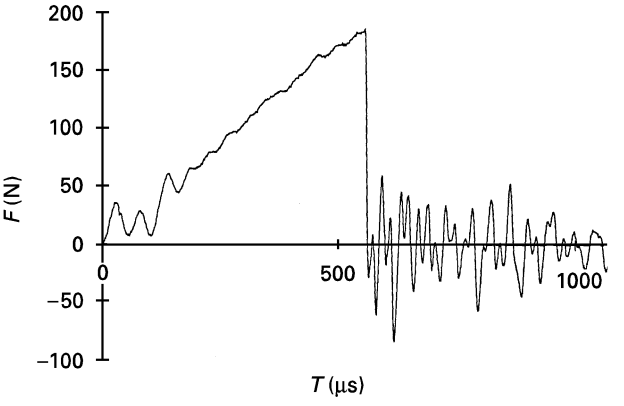

Figure 3 Typical falling weight Charpy impact load-time curve of the pure PP specimen.

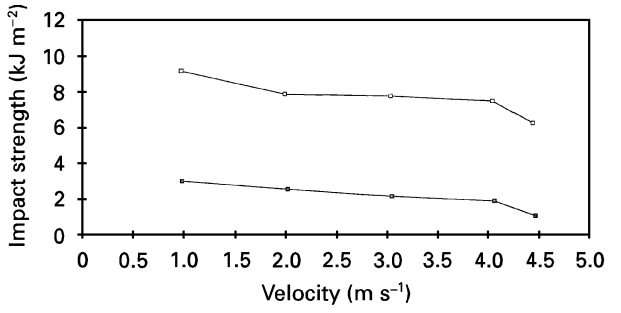

Figure 4 Falling weight impact strength of pure PP and pure PA6 specimens versus impact velocity. (□) PA; (■) PP.

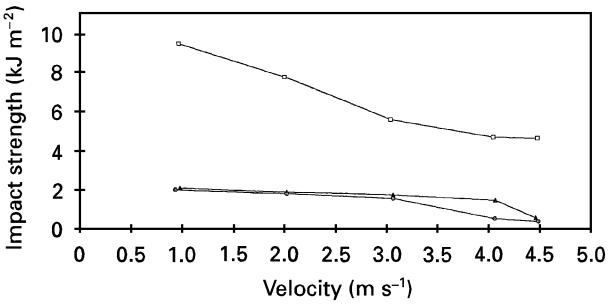

Figure 5 Falling weight impact strength of PP-PA6 blends versus impact velocity. (△) PP-PA 80:20; (○) PP-PA 50:50; (□) PP-PA 20:80.

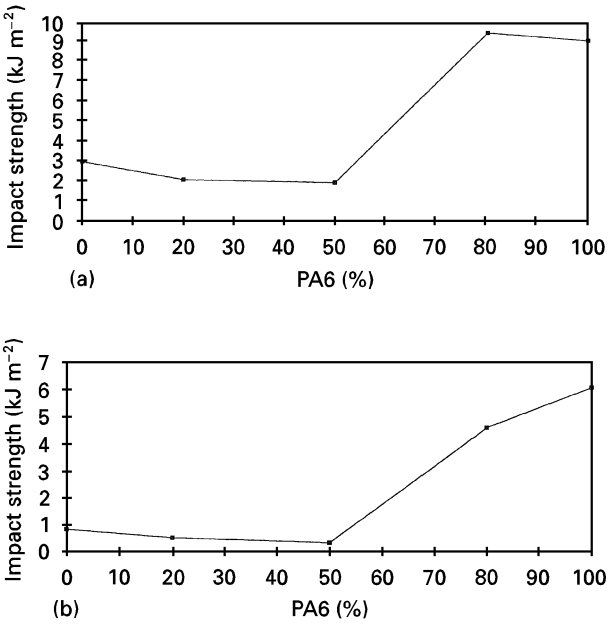

Figure 6 Falling weight impact strength of PP-PA6 blends versus PA content at impact velocities of (a) 1 and (b) 4.05 m s^{-1}.

As the blend morphology plays an important role in determining the mechanical properties of PP–PA6 blends, it is necessary to examine the fracture surfaces of the specimens after impact tests. Fig. 7a shows a low magnification SEM fractograph of a PP impact specimen tested at 1 m s^{-1}. A higher magnification of the region next to the notch is shown in Fig. 7b. From Fig. 7a, one can see the formation of a semi-circular fracture induction zone [13] as localized plastic deformation of the matrix occurs near this region. The size of this zone depends dramatically on the impact velocity. The size of the zone apparently decreases with the impact velocity. As the impact velocity is increased to 4.4 m s^{-1}, the fracture induction zone of the PP specimen disappears, and the fractograph shows brittle cleavage type failure only (Fig. 7c), because the formation of the fracture induction zone is associated with the absorption of energy during impact tests. Thus the larger the area of the induction zone, the higher the impact strength of the material. It appears that the SEM fractographs correlate well with the impact test results, i.e. the impact strength of the PP specimen tends to increase with decreasing impact velocity as shown in Fig. 4.

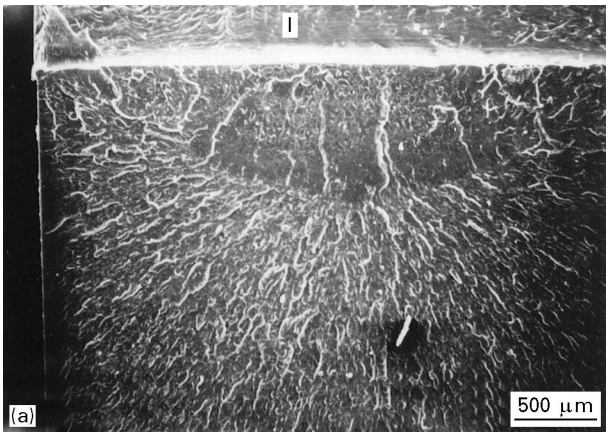

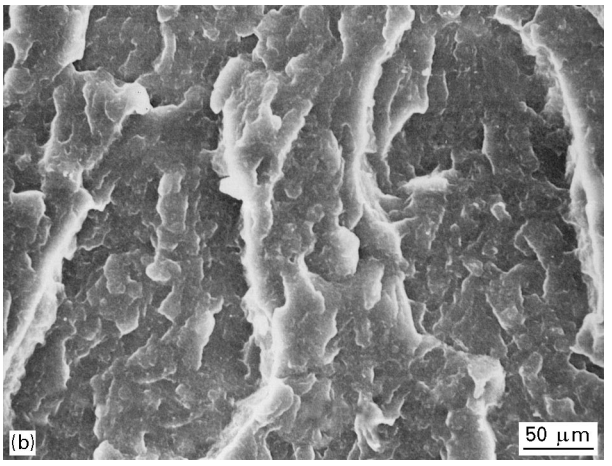

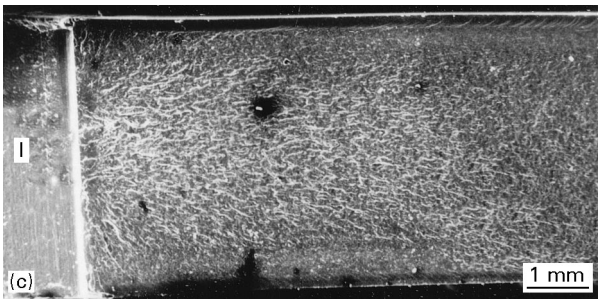

Figure 7 (a) Low magnification SEM fractograph of pure PP specimen after impact test at 1 m s^{-1}; (b) A higher magnification micrograph of (a) taken near the crack initiation area; (c) Low magnification SEM fractograph of pure PP specimen after impact test at 4.4 m s^{-1}. I denotes the notch.

Fig. 8a shows an SEM fractograph taken near the fracture induction zone of the PP–PA 80:20 blend, whereas Fig. 8b is an SEM micrograph taken from the fast fracture region of this polymer blend. From Fig. 8b, plastic deformation of the matrix (PP) does not occur in the fast fracture region as the micrograph taken from this region represents the original size and shape of the dispersed PA phase. It is evident in Fig. 8b that the PA domains are hardly recognized due to the diffused phase boundary. This implies the strong compatibilization of maleic anhydride on the blends at this composition. Such fracture morphology is also observed in the region next to the notch (Fig. 8a).

We now consider the morphology of PP–PA 50:50 blend. Fig. 9a shows an SEM fractograph of PP–PA 50:50 blend taken near the fast fracture region. One can see that the dispersed droplets are well bonded to

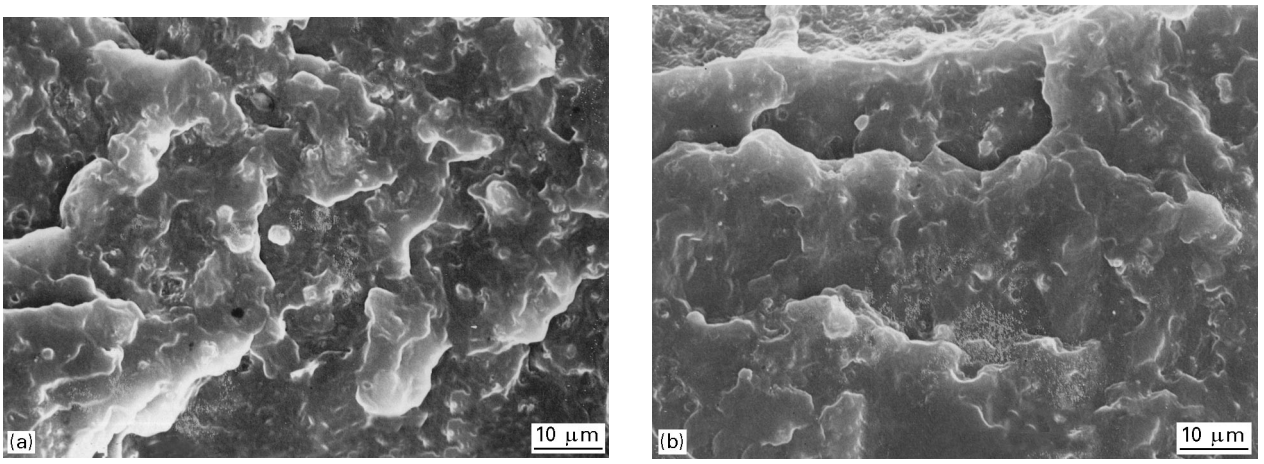

Figure 8 SEM fractographs of the PP-PA 80:20 blend taken near (a) crack initiation zone and (b) fast fracture region after impact test at $1\,m\,s^{-1}$.

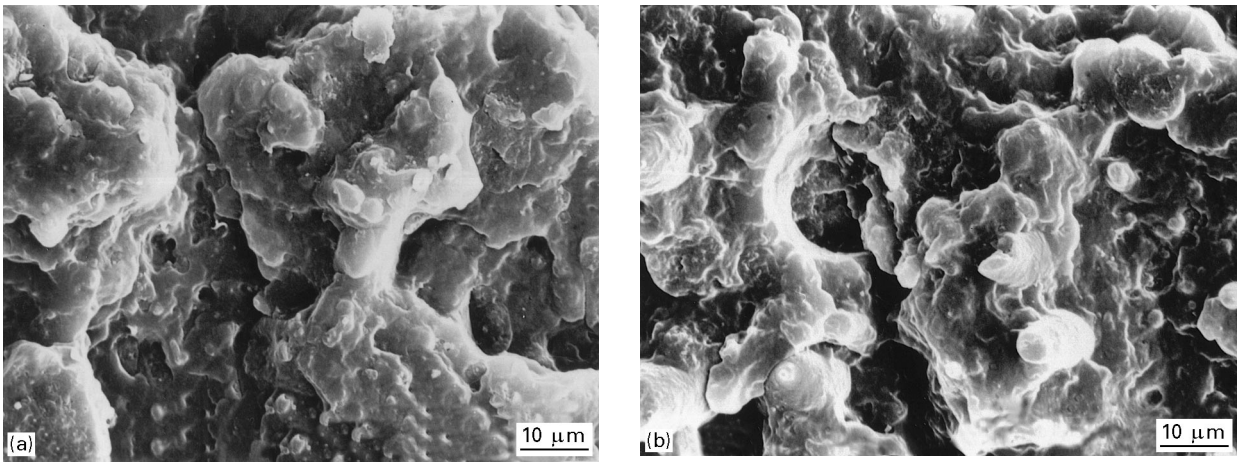

Figure 9 SEM fractographs of PP-PA blends taken near (a) fast fracture region and (b) crack initiation zone after impact test at $1\,m\,s^{-1}$.

the matrix. The phase boundary is almost indistinguishable in this blend. Moreover, the SEM fractograph also reveals that the crack initiation zone also exhibits a similar fracture feature (Fig. 9b). As the viscosity of PA is about three times larger than that of PP [5], we can assign the dispersed droplets as PP domains whereas the continuous matrix is PA phase according to Taylor's theory [14]. This theory states that the dispersed particles can be deformed only when their viscosity does not exceed that of the matrix [14].

Fig. 10a is a low SEM micrograph of the PP–PA 20:80 blend showing the entire fracture surface of the specimen. A shear zone in the outer skin area can be observed in this fractograph apparently. Moreover, the fracture surface is very rough next to the crack initiation zone. Fig. 10b and c shows SEM fractographs taken near the crack initiation zone and fast fracture region, respectively. It can be seen from Fig. 10c than fine PP domains with sizes of about 0.5–1 μm are dispersed within the PA matrix. The PP domains remain intact with the PA matrix indicating that good adhesion exists between the two phases. Thus the maleic anhydride grafted PP compatibilizer appears to be very effective in reducing the PP dispersed particles in this blend. A good compatibilizer generally should reduce the interfacial energy between phases to permit fine dispersion in the melt and to promote good adhesion between the phases [10, 15]. The interaction of maleic anhydride grafted PP with PA probably occurs due to hydrogen bonding involving the amine end group of PA and the functional group of the modified PP [5, 6].

From Fig. 10b, debonding of the PP domains from the PA matrix is observed in the region next to the notch. The PA matrix is highly cold drawn into a fibrous structure indicating that extensive plastic deformation of the matrix occurs within the crack initiation region. Furthermore, deformed matrix tips adhere to the dispersed droplets (Fig. 10d). Thus debonding of the PP dispersed phase from the PA matrix must dissipate a considerable amount of the input impact energy due to the fact that the PP domains adhere strongly to the matrix. As debonding and cavitation occur simultaneously at the PP–PA interface, which relieve the plane-strain constraint and promote massive shear deformation in the PA matrix, this plastic deformation also absorbs a large amount of impact energy. Therefore, we can expect the PP–PA 80:20 blend to exhibit the highest impact strength among the PP–PA blends investigated. On the basis of SEM observations, it appears that improvement in the

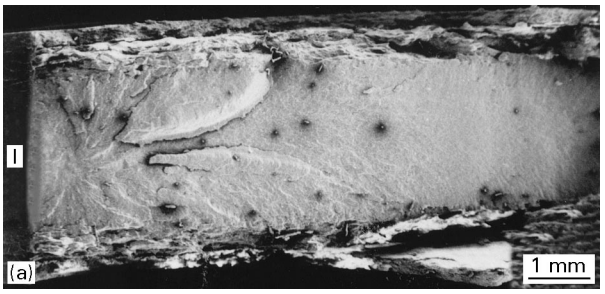

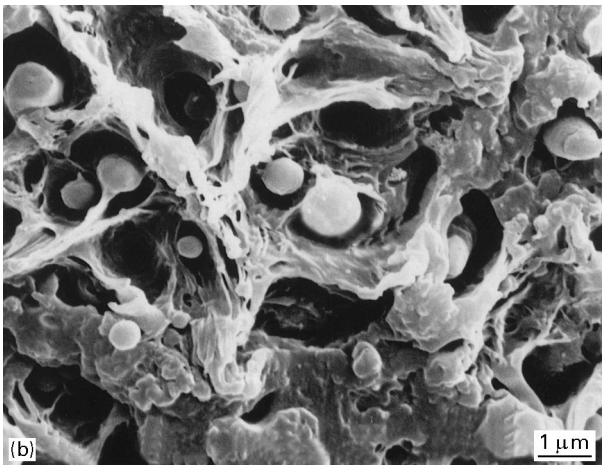

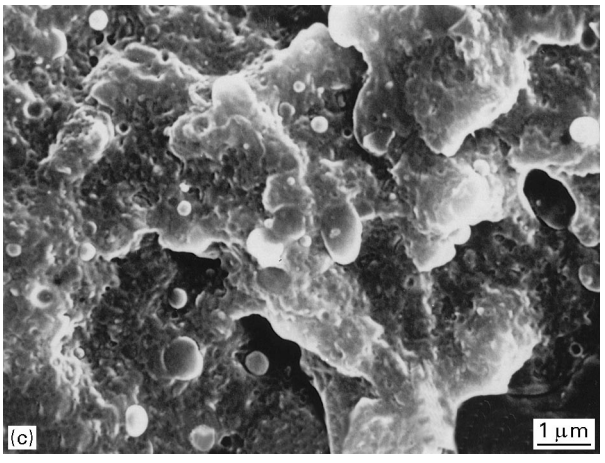

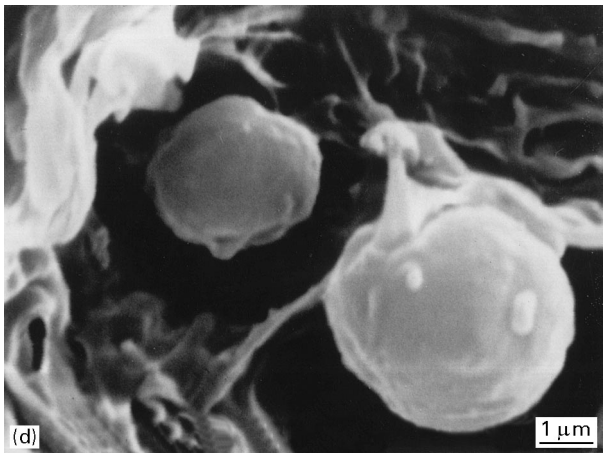

Figure 10 (a) Low magnification SEM fractograph of PP-PA 20:80 blend showing shear deformation in the outer skin of specimen after impact test at 1 ms^{-1}. I denotes the notch; (b) and (c) are higher magnification fractographs taken in the regions next to the notch and fast fracture area, respectively; (d) SEM micrograph showing debonding and cavitation at PP-PA interface.

impact properties of the blends as a function of PA content may take place when the continuous PP phase is replaced by a continuous PA phase: and this continuous PA phase should be heavily cold drawn during plastic deformation. The SEM observations are in good agreement with the results of impact tests as shown in Fig. 6.

4. Conclusions

1. A series of PP–PA6 blends compatibilized by maleic anhydride grafted polypropylene was prepared using a twin screw extruder followed by injection moulding.

2. The tensile and falling weight impact tests showed that the Young's modulus, tensile strength and impact energy of the blends tended to increase with increasing PA concentration.

3. The impact strength was better in blends when the PA content reached 80 wt %. SEM fractographs revealed that the higher impact resistance of the PP–PA 20:80 blend was caused by the cold drawn PA matrix and debonding–cavitation at the PP–PA interface.

References

1. B. R. LIANG, J. L. WHITE, J. E. SPRUIELL and B. C. GOSWAMI, *J. Appl. Polym. Sci.* **28** (1983) 2011.
2. H. K. CHUANG and C. D. HAN, *ibid.* **30** (1985) 165.
3. P. VAN GHELUWE, B. D. FAVIS and J. P. CHALIFOUX, *J. Mater. Sci.* **23** (1988) 3910.
4. A. R. PADWA, *Polym. Eng. Sci.* **32** (1992) 1703.
5. F. P. LAMANTIA, *Adv. Polym. Technol.* **12** (1993) 47.
6. J. DUVALL, C. SELLITTI, C. MYERS, A. HILTNER and E. BAER, *J. Appl. Polym. Sci.* **52** (1994) 195.
7. B. KNOBEL, J. P. VILLEMAIRE and J. F. AGASSANT, *Int. Polym. Processing* **9** (1994) 119.
8. B. D. FAVIS, J. P. CHALIFOUX and P. VAN GHELUWE, Society of Plastics Engineers Technical Paper 33 (SPE, Brookfield, Connecticut, USA, 1987) p. 1326.
9. F. IDE and A. HASEGAWA, *J. Appl. Polym. Sci.* **18** (1974) 963.
10. J. DUVALL, C. SELLITTI, V. TOPOLKARAEV, A. HILTNER, E. BAER and C. MYERS, *Polymer* **35** (1994) 3948.
11. Z. LIANG and H. L. WILLIAMS, *J. Appl. Polym. Sci.* **44** (1992) 699.
12. S. S. DAGLI, M. XANTHOS and J. A. BIESENBERGER, *Polym. Eng. Sci.* **34** (1994) 1720.
13. S. C. TJONG, J. S. SHEN and R. K. Y. LI, *Polymer* **37** (1996) 2309.
14. G. I. TAYLOR, *Proc. R. Soc.* **A 146** (1934) 501.
15. R. ARMAT and A. MOET, *Polymer* **34** (1993) 977.

Received 28 May 1996
and accepted 26 February 1997